Title
Association of p60c-src with endosomal membranes in mammalian fibroblasts.

Journal
Journal of Cell Biology, 118(2)

ISSN
0021-9525

Authors
Kaplan, KB
Swedlow, JR
Varmus, HE
et al.

Publication Date
1992-07-15

DOI
10.1083/jcb.118.2.321

Peer reviewed

Association of p60$^{c\text{-}src}$ with Endosomal Membranes in Mammalian Fibroblasts

Kenneth B. Kaplan,* Jason R. Swedlow,‡ Harold E. Varmus,*§ and David O. Morgan‖

Departments of *Microbiology and Immunology, §Biochemistry and Biophysics, and ‖Physiology, and ‡Graduate Program in Biophysics, University of California, San Francisco, California 94143

Abstract. We have examined the subcellular localization of p60$^{c\text{-}src}$ in mammalian fibroblasts. Analysis of indirect immunofluorescence by three-dimensional optical sectioning microscopy revealed a granular cytoplasmic staining that co-localized with the microtubule organizing center. Immunofluorescence experiments with antibodies against a number of membrane markers demonstrated a striking co-localization between p60$^{c\text{-}src}$ and the cation-dependent mannose-6-phosphate receptor (CI-MPR), a marker that identifies endosomes. Both p60$^{c\text{-}src}$ and the CI-MPR were found to cluster at the spindle poles throughout mitosis. In addition, treatment of interphase and mitotic cells with brefeldin A resulted in a clustering of p60$^{c\text{-}src}$ and CI-MPR at a peri-centriolar position. Biochemical fractionation of cellular membranes showed that a major proportion of p60$^{c\text{-}src}$ co-enriched with endocytic membranes. Treatment of membranes containing HRP to alter their apparent density also altered the density of p60$^{c\text{-}src}$-containing membranes. Similar density shift experiments with total cellular membranes revealed that the majority of membrane-associated p60$^{c\text{-}src}$ in the cell is associated with endosomes, while very little is associated with plasma membranes. These results support a role for p60$^{c\text{-}src}$ in the regulation of endosomal membranes and protein trafficking.

p60$^{c\text{-}src}$ is a member of a family of cytoplasmic tyrosine kinases that are associated with cellular membranes and are thought to be involved in signal transduction events underlying growth control (for review see Cooper, 1989). The normal function of p60$^{c\text{-}src}$ is not clear, although studies of mutant forms of the protein (e.g., the viral transforming protein p60$^{v\text{-}src}$) have implicated p60$^{c\text{-}src}$ in the control of cell growth and proliferation. On the other hand, p60$^{c\text{-}src}$ is expressed at high levels in terminally differentiated cells such as platelets and neurons (Cotton and Brugge, 1983; Golden et al., 1986). In addition, p60$^{c\text{-}src}$ is activated during mitosis in fibroblasts and thus may mediate certain mitotic events (Chackalaparampil and Shalloway, 1988; Morgan et al., 1989; Shenoy et al., 1989). Finally, a homozygous disruption of the c-src gene in mice is not lethal, but instead leads to defects in bone remodeling (probably as a result of defective osteoclast function) (Soriano et al., 1991).

Clues about p60$^{c\text{-}src}$ function have been obtained from studies of the subcellular location of src proteins. Immunofluorescence and biochemical fractionation studies have suggested that both p60$^{c\text{-}src}$ and p60$^{v\text{-}src}$ are localized to perinuclear and plasma membranes, while transforming proteins have also been found in association with adhesion plaques (Courtneidge et al., 1980; Resh and Erikson, 1985; Rohrschneider, 1980). Immunofluorescence studies of p60$^{c\text{-}src}$ have also revealed a punctate staining pattern that is dependent on membrane attachment domains in the amino-terminal region of the protein (Kaplan et al., 1990). This punctate pattern is characteristic of membrane vesicles, suggesting that p60$^{c\text{-}src}$ is associated with cellular membranes distinct from the plasma membrane. Although these membranes remain uncharacterized, analysis of p60$^{c\text{-}src}$ over expressed in 3T3 cells indicates a possible connection with endosomal membranes (David-Pfeuty and Nouvian-Dooghe, 1990). In addition, recent efforts to localize p60$^{c\text{-}src}$ in differentiated PC12 cells and neuroendocrine cells have shown that a significant proportion of p60$^{c\text{-}src}$ is associated with an endosomally derived population of vesicles (Linstedt et al., 1992; Grandori and Hanafusa, 1988).

To gain insight into the normal role of p60$^{c\text{-}src}$, we have used high resolution immunofluorescence analysis and biochemical fractionation to characterize the nature of p60$^{c\text{-}src}$-containing membranes. Our results indicate that p60$^{c\text{-}src}$ is mainly associated with endosomal membranes and is particularly enriched in a population of late endosomes.

Materials and Methods

Cells

The RTCS cell line was derived from a Rat-1 cell line infected with a retroviral construct expressing chicken p60$^{c\text{-}src}$ (Morgan et al., 1989) and expresses ~7.5-fold more p60$^{c\text{-}src}$ than the parental Rat-1 cell line (determined by Western blot: our own unpublished observations). In some experiments, we used cell lines derived from the spontaneous immortalization of mouse embryo fibroblasts isolated from mice heterozygous or homozygous for a disruption of the c-src gene (cells kindly provided by P. Soriano, Bay-

lor College of Medicine, Houston, TX). Cells were cultured in DME H-16 with 10% FCS at 37°C in 5% CO_2.

Antibodies

mAbs against $p60^{c\text{-}src}$ were kindly provided by Joan Brugge (University of Pennsylvania, Philadelphia, PA) (mAb327) and Sara Courtneidge (mAb2-17) (Lipsich et al., 1983). Polyclonal rabbit sera against the cation-independent mannose 6-phosphate receptor (CI-MPR) were kindly provided by Peter Lobel (Rutgers University, New Brunswick, NJ) and Bill Brown (Cornell University, Ithaca, NY). mAbs against *cis/medial*-Golgi markers (10E6 and 8B3) were also kindly provided by Bill Brown (Cornell University). Antibodies against BiP binding protein were obtained from David Bole (University of Michigan). mAb against β-tubulin (tub2.1) was purchased from Sigma Chemical Co. (St. Louis, MO). Texas red and fluorescein-labeled secondary anti-rabbit and anti-mouse antibodies were purchased from Accurate Chemical and Scientific Corp. (Westbury, NY) and used at recommended dilutions.

Immunofluorescence

Cells were plated in six-well plates on glass coverslips 18–36 h before analysis. After specified treatments, cells were washed twice with PBS and then fixed for 20 min at 20°C in freshly made 3.7% paraformaldehyde/PBS (Polysciences Inc. Warrington, PA). Fixed cells were washed twice with PBS and permeabilized with 0.1% Triton X-100 in PBS. Cells were rinsed and then blocked in PBS + 0.2% gelatin + 0.02% NaN_3. Primary antibodies were used at the following dilutions for 20 min at 20°C in a humidified chamber: mAb 327 (1 mg/ml): 1/100; tub2.1: 1/200; CI-MPR; 1/200; mAb 2-17: 1/200; mAb 10E6/8B3: undiluted cell culture supernatants. Coverslips were then treated with secondary antibodies at the appropriate dilutions. Endogenous levels of $p60^{c\text{-}src}$ in Rat-1 fibroblasts were detected with an unlabeled rabbit anti-mouse antibody (used at 1 μg/ml) followed by goat anti-rabbit antibody labeled with Texas red. Controls performed with only secondary and tertiary antibodies resulted in negligible signals. Coverslips were washed in PBS + 0.2% gelatin + 0.02% NaN_3, followed by PBS, and finally incubated in Hoechst stain (No. 33258, Sigma Chemical Co.) for 5 min at 20°C before mounting in a solution of 3% *n*-propyl gallate in glycerol. The specificity of the $p60^{c\text{-}src}$ signal was demonstrated by adding excess amounts of purified baculovirus-produced chicken $p60^{c\text{-}src}$ (Morgan et al., 1991).

In costaining experiments with mAb tub2.1 and mAb 327, mAb tub2.1 was directly labeled with Texas red (Harlow and Lane, 1988). The labeled mAb tub2.1 was separated from unincorporated Texas red by gel filtration on a G-50 Sephadex column. Staining with mAb 327 was carried out as above and followed by an additional fixation step before incubation with mAb tub2.1-Texas red. This process fixed the anti-mouse antibody and ensured no cross-reactivity between the fluorescein-conjugated anti-mouse antibody and the mAb tub2.1. No tubulin staining was seen in the fluorescein channel, indicating that there was no interaction between fluorescein-labeled anti-mouse antibodies and mAb tub2.1.

Three-dimensional Optical Sectioning Microscopy and Image Processing

Data were recorded using a Peltier-cooled charge-coupled device (CCD) camera (Photometrics Ltd., Tucson, AZ) mounted on an inverted microscope (Olympus Corp., Lake Success, NY). Images were collected with a 60×/1.4 oil immersion lens (Olympus Corp.); the effective CCD pixel size was 0.074 μm × 0.074 μm. Optical sections were recorded at 0.2 μm intervals. Multiple-wavelength data were collected using a single dichroic mirror designed for DAPI (4',6-diamidino-2-phenylindole), fluorescein and Texas red wave lengths (Omega Optical Inc., Brattleboro, VT). This prevented large registration errors between images recorded with different wavelengths of light (Hiraoka et al., 1991). Excitation and barrier filters were mounted on motorized wheels; wavelength switching and all other aspects of microscope data collection were controlled by a MicroVax III workstation (Hiraoka et al., 1990, 1991). Once the three-dimensional data stacks were recorded, each was corrected for any photobleaching and lamp intensity variations which occurred during data collection (Paddy et al., 1990). Out-of-focus information was removed from each data stack by a three-dimensional, iterative deconvolution program with a non-negativity constraint (Agard et al., 1989). This method moves photons from their recorded positions (out-of-focus) to their points of origin without subtracting any of the information in the images. After the out-of-focus information was removed, projections representing the three-dimensional reconstruction of individual optical sections through the entire cell were generated. Data are presented both as projections of the entire set of optical sections, or as individual optical sections where noted. Some data are presented as unprocessed images recorded by the CCD camera.

Membrane Isolation and Fractionation

RTCS cells were plated 18–36 h before harvesting and allowed to reach a final confluency of 75–85%. Cells were loaded with HRP (Sigma Chemical Co.) (7.5–10 mg/ml in DME H-16, 10% FCS) at 37°C for 30 min (sufficient to saturate the endocytic pathway in these cells). Cells were chilled on ice, washed 4 times in ice-cold PBS and then scraped into homogenization buffer (20 mM Hepes, pH 7.4, 150 mM KCl, 2 mM $MgCl_2$, 10 mM EDTA, 1 mM PMSF, 1 μg/ml leupeptin, 10 μg/ml pepstatin, 0.1 mg/ml soybean trypsin inhibitor, 1 U/ml aprotinin, 0.25 M sucrose). Cells were homogenized in a 2-ml dounce (Wheaton Inds., Millville, NJ) with an A pestle for 30–40 strokes. After homogenization, nuclear membranes were pelleted for 10 min at 2,000 *g* in an SS-34 rotor (Sorvall, Dupont, Wilmington, DE) at 4°C. The postnuclear supernatant (S1) was collected and loaded over a 62% sucrose cushion and spun at 100,000 *g* in an SW50.1 rotor for 35 minutes at 4°C. Membranes at the interface were resuspended in the sucrose cushion (adjusted to 45% sucrose) and placed at the bottom of a sucrose step gradient consisting of 45, 32, and 18% steps. The gradient was centrifuged at 35,000 rpm in an SW50.1 rotor for 60 min at 4°C. The 18/32% interface was collected with a 23-gauge needle and a 2.5-ml syringe. The remaining fractions were collected from the top of the gradient with a pasteur pipette and analyzed for $p60^{c\text{-}src}$ and membrane markers.

Under these homogenization conditions (30–40 strokes) 30–40% of HRP activity was left in the nuclear pellet and plasma membranes were mainly observed in the 45% sucrose fraction. Harsher homogenization conditions (80 strokes) left <1% of the total HRP activity in the nuclear pellet and the majority of plasma membranes were observed in the 32% and interface (18/32%) fractions on sucrose gradients.

To analyze the 18/32% sucrose interface on percoll gradients, the fraction was mixed into a 27% percoll solution (8.5% sucrose) and centrifuged over a 62% sucrose cushion in a 50Ti rotor at 16,000 rpm for 60 min at 4°C. Fractions were collected from the bottom of the tube and assayed for membrane markers and $p60^{c\text{-}src}$ by immunoblotting.

Membrane markers were assayed as follows. The plasma membrane marker alkaline diphosphoesterase I (ADPE I) was measured with thymidine-5'-monophosphate-*p*-nitrophenyl ester (Sigma Chemical Co.) and assayed using a Beckman fluorometer at excitation 355 nM and emission 455 nM (Poole et al., 1983). The lysosomal marker β-hexosaminidase was measured with the fluorometric substrate 4-methyl umbelliferyl-*N*-acetyl-β-D-glucosaminide (Sigma Chemical Co.) and samples were read on a Beckman fluorometer at excitation 350 nM and emission 450 nM (ref). The Golgi marker galactosyl transferase was measured by incorporation of UDP-[3H]-galactose (Amersham Corp., Arlington Heights, IL) into BSA (Aoki et al., 1990). HRP activity was measured using *o*-dianisidine (Sigma Chemical Co.) prepared at 0.11 μg/ml in PBS, pH 5.0, 0.1% Triton X-100. Activity was measured at OD_{460} at several time points (or at several volumes of extract) to ensure linearity of the assay.

Density Shift and DAB Cytochemistry

HRP-containing membranes from the 18/32% interface or from the P100 fraction (isolated under relatively harsh homogenization conditions; see above) were treated with DAB in homogenization buffer to a final concentration of 6 μg/ml. 10 μl of 30% H_2O_2 was added and the mixture incubated in the dark at 0°C for 10 min. After treatment, membranes were loaded on another sucrose gradient or a percoll gradient as described above, centrifuged, and analyzed for $p60^{c\text{-}src}$ and membrane markers. In control experiments no density shift was observed if DAB or H_2O_2 were added separately.

To inhibit HRP entry in some experiments, cells were chilled on ice and cold media containing HRP was incubated with the cells at 0°C for 20 min. Half of the cells were placed at 37°C for 40 min. Both sets of plates were then washed and membranes harvested as above. DAB cytochemistry was carried out and fractions from percoll gradients were analyzed for $p60^{c\text{-}src}$ and membrane markers.

1. *Abbreviations used in this paper*: ADPE I, alkaline diphosphoesterase I; BFA, brefeldin A; CCD, charge-coupled device; CI-MPR, cation-independent mannose 6-phosphate receptor; MTOC, microtubule organizing center: TGN, *trans*-Golgi network.

Monitoring of plasma membranes by surface iodination was performed with cells loaded for 30 min at 37°C with HRP. Cells were chilled on ice, washed 4 times with ice cold PBS and then dislodged from the plate using PBS + 1 mM EDTA. Cells were extensively washed in ice cold PBS and then labeled using sulfo-SHPP (Pierce Chemical Co. Rockford, IL) labeled with iodobeads (Thompson et al., 1987). Free ^{125}I counts were washed out of the cells using ice cold PBS. Membranes were isolated and DAB cytochemistry was performed and analyzed as above.

Immunoprecipitation and Immunoblotting

For immunoprecipitating p60$^{c\text{-}src}$, fractions were diluted two times with homogenization buffer and adjusted to 1% Triton X-100. mAb 327 was added and incubated at 4°C for 1–4 h. Protein A-sepharose conjugated to a rabbit anti-mouse antibody was added (50 μl/fraction of 50% slurry) and incubated at 4°C for 1–2 h. After one wash with homogenization buffer + 1% Triton X-100, protein A-sepharose beads were boiled in loading buffer, and supernatants were loaded onto 10% PAGE gels. After electrophoresis, proteins were transferred to nitrocellulose on an electroblot apparatus (Bio-Rad Laboratories, Cambridge, MA), and blots were blocked in 2% BSA for 1 h at 20°C. Blots were incubated in mAb327 (1 μg/ml) at 4°C for 18–24 h. Secondary ^{125}I-labeled goat anti-mouse IgG (New England Nuclear, Boston, MA) was incubated for 1–4 h at 4°C and the blot washed and autoradiography carried out at −70°C. Bands were cut from the blot and counted to measure relative p60$^{c\text{-}src}$ signals. In some experiments, HRP-linked goat anti-mouse IgG (Amersham Corp.) was detected with a chemi-luminescence procedure as described for the Amersham ECL detection system. To recognize antibodies against the CI-MPR, HRP-linked goat anti-rabbit antibodies (Amersham Corp.) were used in the chemi-luminescence protocol.

Results

Co-staining of p60$^{c\text{-}src}$ with Late Endosomes at the Microtubule Organizing Center

Rat-1 fibroblasts over-expressing chicken p60$^{c\text{-}src}$ (RTCS cell line) were analyzed by indirect immunofluorescence with a mAb against p60$^{c\text{-}src}$ (mAb 327). To enhance resolution, immunofluorescence was recorded with an optical sectioning microscope and both individual optical sections and three-dimensional reconstructions of the images were analyzed. Two general populations of p60$^{c\text{-}src}$ were apparent: a granular staining throughout the cytoplasm and a concentrated staining adjacent to the nucleus (Fig. 1 *A*). Staining with a different mAb against p60$^{c\text{-}src}$ (mAb 2-17) demonstrated a similar staining pattern, and signals with either antibody were blocked by addition of purified chicken p60$^{c\text{-}src}$ produced with the baculovirus expression system (Morgan et al., 1991) (data not shown).

Staining with antibodies against tubulin revealed that p60$^{c\text{-}src}$ co-localizes with the microtubule organizing center (MTOC), the region of the cell where many membranous organelles are located (Fig. 1 *B*). The concentration of p60$^{c\text{-}src}$ at the MTOC was not simply because of the increased cell thickness in this region of the cell, as analysis of optical sections showed a distinct region of staining along the vertical axis of the cell where p60$^{c\text{-}src}$ is concentrated (Fig. 1 *C*). In addition, p60$^{c\text{-}src}$ concentrated at the MTOC co-stains with individual cellular microtubules when optical sections from cells stained with antibodies against tubulin (Fig. 1 *D*) are compared to the identical sections stained with antibodies against p60$^{c\text{-}src}$ (Fig. 1 *C*). This staining pattern is also not because of the over-expression of chicken p60$^{c\text{-}src}$ in these cells, as endogenous p60$^{c\text{-}src}$ in Rat-1 fibroblasts exhibited an identical pattern (Fig. 1 *F*). In addition, the depolymerization of cellular microtubules with the drug nocodazole dispersed p60$^{c\text{-}src}$ (Fig. 1 *E*) and suggested a direct association with the MTOC. P60$^{c\text{-}src}$ rapidly returned to the peri-nuclear region of the cell upon removal of nocodazole and the repolymerization of cellular microtubules (data not shown).

P60$^{c\text{-}src}$ is myristylated at its NH_2-terminus (Buss and Sefton, 1985), and the myristylation signal is necessary but not sufficient for association with cellular membranes (Kaplan et al., 1990). To address the issue of whether membrane association of p60$^{c\text{-}src}$ is required for the localization of p60$^{c\text{-}src}$ at the MTOC, we characterized a 3T3 fibroblast cell line expressing p60$^{c\text{-}src}$ in which the second amino acid glycine has been replaced with alanine. In p60$^{v\text{-}src}$, this amino acid change results in a protein that cannot be myristylated and therefore does not associate with cellular membranes (Buff et al., 1986; Kamps et al., 1986). Immunofluorescence analysis of cells expressing p60$^{c\text{-}src}$ containing this substitution showed a diffuse cytoplasmic staining, indicating that membrane attachment is required for localization at the MTOC, as previously suggested (Kaplan et al., 1990) (Fig. 2, *A* and *B*). We also failed to observe the granular cytoplasmic p60$^{c\text{-}src}$ staining pattern, indicating that membrane association is required for this localization as well. To determine whether membrane association alone is sufficient for localization of p60$^{c\text{-}src}$ at the MTOC, we analyzed a membrane-associated fusion protein comprising the first 14 amino acids of p60$^{c\text{-}src}$ fused to pyruvate kinase (Kaplan et al., 1990). When expressed in Rat-1 cells this protein exhibited a punctate staining pattern and did not co-localize with the MTOC (data not shown). We therefore conclude that myristylation is necessary but not sufficient to allow MTOC localization of p60$^{c\text{-}src}$, supporting the notion that there are other domains of p60$^{c\text{-}src}$ that contain information important for localization (Kaplan et al., 1990).

Membrane organelles involved in various secretory and endocytic processes have been localized to the MTOC. To identify candidate membranes that contain p60$^{c\text{-}src}$, co-localization studies were performed with a number of antibodies against markers of specific membrane compartments. The Golgi compartment was identified with several markers, including fluorescein-conjugated wheat germ agglutinin and two mAbs, 10E6 and 8B3, specific for *cis/medial*-Golgi elements (Wood et al., 1991). These markers stained a perinuclear region of the cell that was distinct from p60$^{c\text{-}src}$, suggesting that p60$^{c\text{-}src}$ is not found in *cis/medial*-Golgi membranes (Fig. 2 *C*). Similarly, staining of the ER with antibodies against BiP (Bole et al., 1989) and staining of lysosomes with antibodies against lgp120 (Lewis et al., 1985) revealed that these two membrane compartments are clearly distinct from p60$^{c\text{-}src}$ at the MTOC (data not shown).

In contrast, staining with antibodies to the CI-MPR, a marker of endosomes and *trans*-Golgi network (TGN), revealed a striking co-localization with p60$^{c\text{-}src}$ at the MTOC (Fig. 2, *D* and *E*). While all endosomal membranes are believed to contain the CI-MPR, the CI-MPR–positive endosomes located at the MTOC represent vesicles at a late stage in the endocytic pathway (late endosomes or pre-lysosomes) (Messner and Kreis, 1989). CI-MPR–positive vesicles also require intact microtubules for their localization, unlike early endosomes (K. Kaplan, unpublished observations) (Matteoni et al., 1987). Thus, our results suggest that p60$^{c\text{-}src}$ is associated with membranes at the MTOC that represent a late stage in the endocytic pathway. While no di-

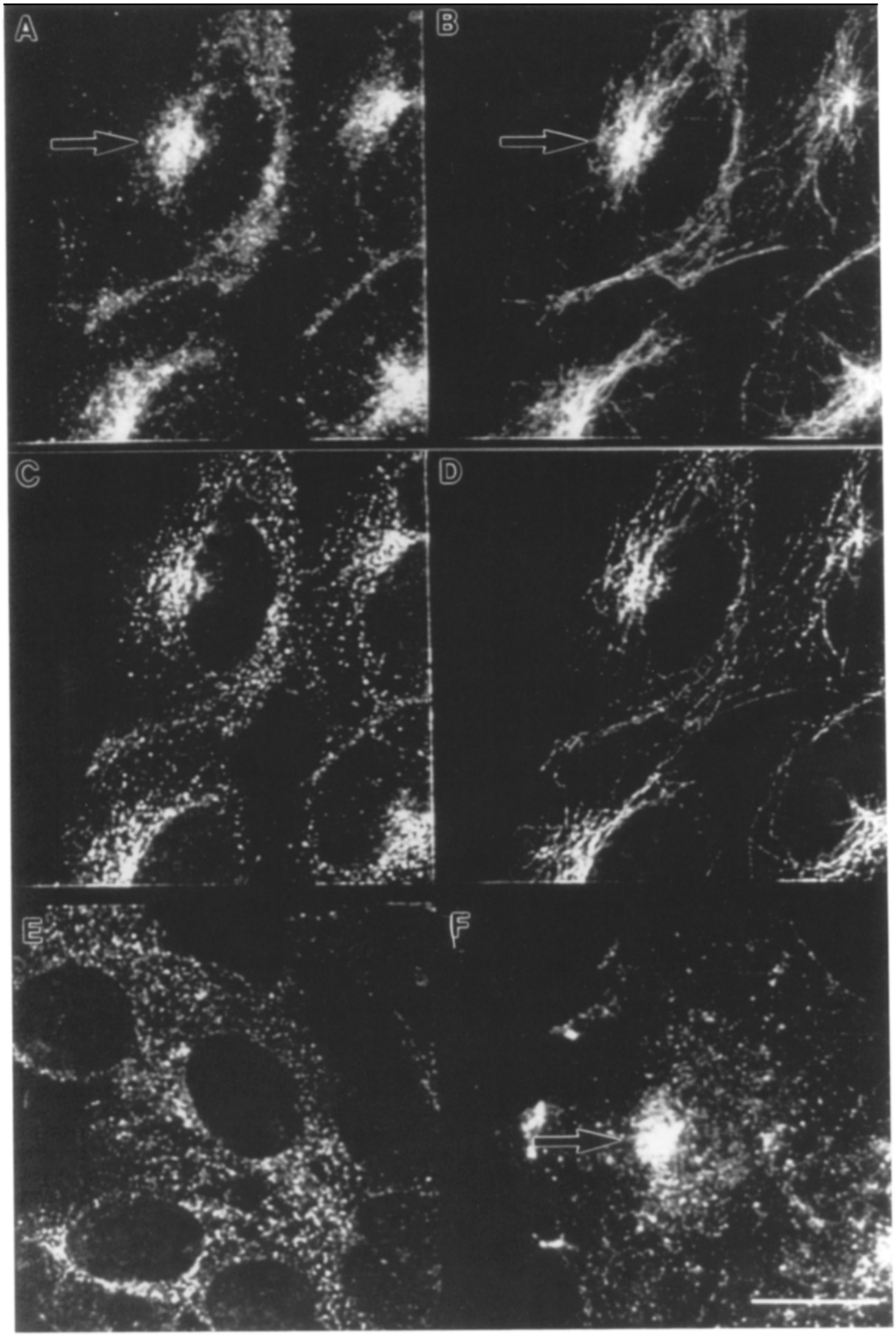
A
B
C
D
E
F

rect attempts were made to distinguish CI-MPR-positive endosomes from CI-MPR-positive TGN, we observed that p60$^{c\text{-}src}$ did not exhibit the tubular staining pattern characteristic of the TGN (data not shown).

P60$^{c\text{-}src}$ and CI-MPR Co-localize after Treatment with BFA

To further analyze p60$^{c\text{-}src}$-containing membranes and to distinguish these membranes from *cis/medial*-Golgi network, we treated cells with brefeldin A (BFA). BFA disrupts the normal distribution of *cis/medial*-Golgi membranes, causing retrograde transport to the ER. This results in a reticular staining pattern when the Golgi apparatus is visualized by immunofluorescence (Lippincott-Schwartz et al., 1989, 1990). In contrast, BFA treatment does not result in the transport of CI-MPR-containing membranes into the ER (Chege and Pfeffer, 1990; Lippincott-Schwartz et al., 1991; Wood et al., 1991). If p60$^{c\text{-}src}$ is associated with CI-MPR-containing late endosomes, then the behavior of p60$^{c\text{-}src}$ and CI-MPR after BFA treatment should be similar, and yet distinct from *cis/medial*-Golgi membranes.

Consistent with previous findings, we found that after BFA treatment the Golgi marker 10E6 exhibited a punctate/reticular staining pattern characteristic of ER staining in these cells (Fig. 3 *A*). We also observed that CI-MPR-positive membranes do not enter the ER after BFA treatment. After BFA treatment, both p60$^{c\text{-}src}$ and CI-MPR (Fig. 3, *B* and *C*) formed a tight cluster at the centrosome in a staining pattern that is distinct from *cis/medial*-Golgi membranes. This clustering of membranes containing p60$^{c\text{-}src}$ and CI-MPR at the centrosome is less diffuse than the staining pattern at the MTOC in untreated cells. The clustering occurs after 30 min of BFA treatment, is reversible, and is dependent on intact microtubules, since pretreatment with nocodazole abolishes the effect (data not shown). In untreated populations of fibroblasts, some cells (5–10%) exhibit a similar clustering of p60$^{c\text{-}src}$ and CI-MPR staining at the centrosome, suggesting that the clustering of endosomes in this region can occur in the absence of BFA. These results further support the notion that p60$^{c\text{-}src}$ and the CI-MPR are in a similar cellular compartment that is distinct from the *cis/medial*-Golgi apparatus.

Co-localization of p60$^{c\text{-}src}$ and CI-MPR at the Spindle Poles during Mitosis

The activation of p60$^{c\text{-}src}$ during mitosis suggests that it may play a role in mitosis. Therefore we also examined the localization of p60$^{c\text{-}src}$ in mitotic cells (identified by the state of their chromatin after Hoechst staining; see Materials and Methods). During mitosis, p60$^{c\text{-}src}$ was observed to cluster at the dividing centrosomes (Fig. 4 *A*; *arrows*). Co-staining with anti-CI-MPR clearly demonstrated that the CI-MPR is clustered at the same peri-centriolar position as p60$^{c\text{-}src}$ (Fig. 4 *B*; *arrows*). Reconstructive analysis of three-dimensional optical sections confirmed that p60$^{c\text{-}src}$ staining corresponded to the position of migrating centrioles as determined by tubulin staining (data not shown). Analysis of additional stages of mitosis showed that the peri-centriolar populations of p60$^{c\text{-}src}$ and CI-MPR were present throughout mitosis and appear positioned to form membrane organelles at the MTOC after telophase.

Over-expression of p60$^{c\text{-}src}$ did not affect staining, as similar patterns were apparent when endogenous levels of p60$^{c\text{-}src}$ were examined in Rat-1 cells (Fig. 4, *D* and *E*). The mitotic localization of both CI-MPR and p60$^{c\text{-}src}$ is dependent on a properly formed spindle, since cells treated with nocodazole no longer show pericentriolar staining of p60$^{c\text{-}src}$ or CI-MPR (data not shown). In addition, staining of cells with antibodies specific for the Golgi apparatus revealed that Golgi membranes became vesicularized and were scattered throughout the cell during mitosis as previously reported for HeLa cells (Lucocq and Warren, 1987; Moskalewski and Thyberg, 1990). This contrast between Golgi staining and p60$^{c\text{-}src}$/CI-MPR staining during mitosis provides additional evidence that p60$^{c\text{-}src}$ associates with endosomal membranes and not with *cis/medial*-Golgi elements.

Biochemical Fractionation Reveals that p60$^{c\text{-}src}$ Co-enriches with Endosomal Membranes

We next examined the association of p60$^{c\text{-}src}$ with endosomal membranes by standard cell fractionation techniques. RTCS cells were allowed to internalize the fluid phase marker HRP to label the endocytic compartment. Cellular membranes isolated after a 100,000 *g* spin (P100 pellet) were placed at the bottom of a sucrose step gradient consisting of 45, 32, and 18% steps. Membranes were allowed to float to equilibrium during centrifugation. We determined that the endocytic marker HRP and thus endocytic membranes from these cells were enriched at the 18/32% interphase of the gradient (data not shown). We analyzed the fractions from the gradient by immunoblotting to identify p60$^{c\text{-}src}$ and observed a major peak at the 18/32% interface (Fig. 5 *A*). Based on immunoblots with ^{125}I-labeled antibody, we estimate that 65% of the total p60$^{c\text{-}src}$ on the gradient was at the 18/32% interface (Fig. 5 *B*). A similar pattern of enrichment was observed with cells expressing endogenous levels of p60$^{c\text{-}src}$ (data not shown). The density at the 18/32% interface is characteristic of endosomal membranes and is therefore consistent with the enrichment of p60$^{c\text{-}src}$ with endocytic vesicles. Analysis of markers for membrane compartments demonstrated that fractions enriched for p60$^{c\text{-}src}$ are distinct from lysosomal (data not shown), Golgi apparatus, and plasma membrane markers (Fig. 5, *C–E*), although a small

Figure 1. Co-staining of p60$^{c\text{-}src}$ and the MTOC. Projections comprising multiple optical sections of RTCS fibroblasts (see Materials and Methods) were obtained with mAb 327 against p60$^{c\text{-}src}$ (*A*) and mAb tub 2.1 against tubulin (*B*). Individual optical sections that represent information from the middle of the cells stained with mAb 327 against p60$^{c\text{-}src}$ (*C*) and mAb tub2.1 against tubulin (*D*) are also presented. A single optical section is presented from RTCS cells treated for 30 min with 0.5 μg/ml nocodazole to depolymerize microtubules, and stained with mAb 327 (*E*). A projection of Rat-1 fibroblasts expressing only endogenous c-src was obtained with mAb 327 against p60$^{c\text{-}src}$ (*F*). Endogenous p60$^{c\text{-}src}$ signal was enhanced with a rabbit anti-mouse antiserum (sandwich antibody) between the primary mAb and fluorophore-conjugated secondary antibody. Arrows indicate the MTOC. Bar, 10 μm.

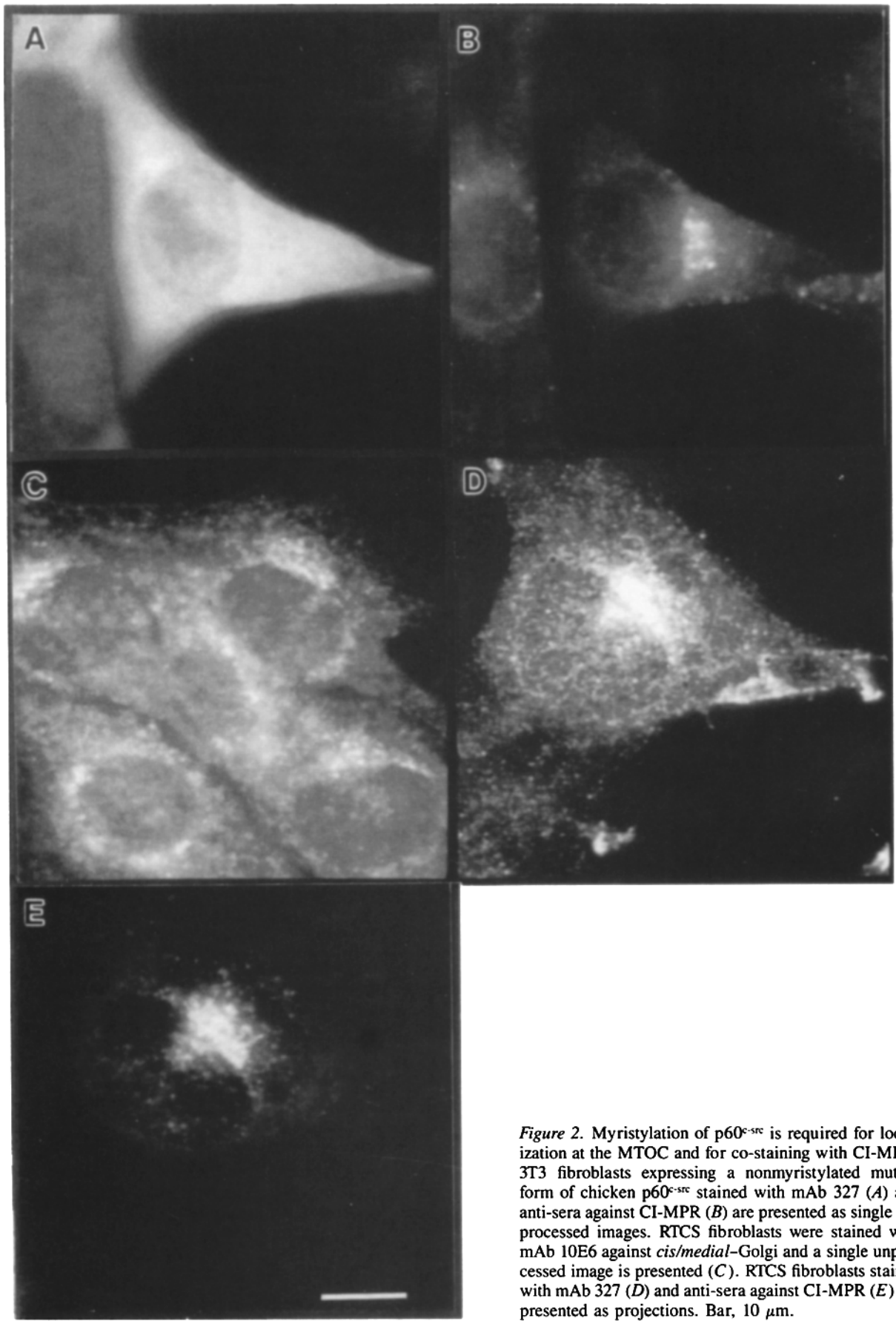

Figure 2. Myristylation of $p60^{c\text{-}src}$ is required for localization at the MTOC and for co-staining with CI-MPR. 3T3 fibroblasts expressing a nonmyristylated mutant form of chicken $p60^{c\text{-}src}$ stained with mAb 327 (*A*) and anti-sera against CI-MPR (*B*) are presented as single unprocessed images. RTCS fibroblasts were stained with mAb 10E6 against *cis/medial*–Golgi and a single unprocessed image is presented (*C*). RTCS fibroblasts stained with mAb 327 (*D*) and anti-sera against CI-MPR (*E*) are presented as projections. Bar, 10 μm.

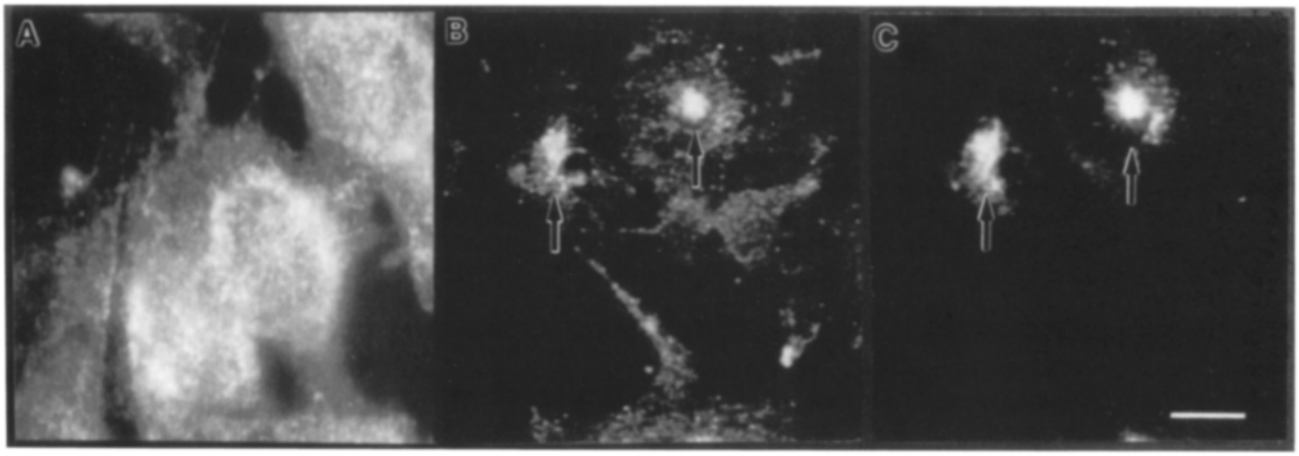

Figure 3. Brefeldin A treatment causes p60$^{c\text{-}src}$ and CI-MPR membranes to cluster at the centrosome. RTCS fibroblasts were treated with 1 μg/ml brefeldin A for 30 min at 37°C and then processed for immunofluorescence. A single unprocessed image of staining with mAb 10E6 against *cis/medial*-Golgi is presented (*A*), while projections of multiple optical sections are presented for staining with mAb 327 against p60$^{c\text{-}src}$ (*B*) and anti-sera against CI-MPR (*C*). Arrows indicate clustered p60$^{c\text{-}src}$ and CI-MPR staining at the centrosome. Bar, 10 μm.

amount of plasma membrane marker was found at the 18/32% interface (see Materials and Methods).

P60$^{c\text{-}src}$ was sometimes observed in the 45 and 32% fractions. To address whether this material was membrane-associated, each fraction from the sucrose step gradient was diluted to a final concentration of 8.5% sucrose, pelleted at 100,000 *g* and the pellet analyzed for p60$^{c\text{-}src}$ by immunoblotting. Approximately 90% of the p60$^{c\text{-}src}$ in these frac-

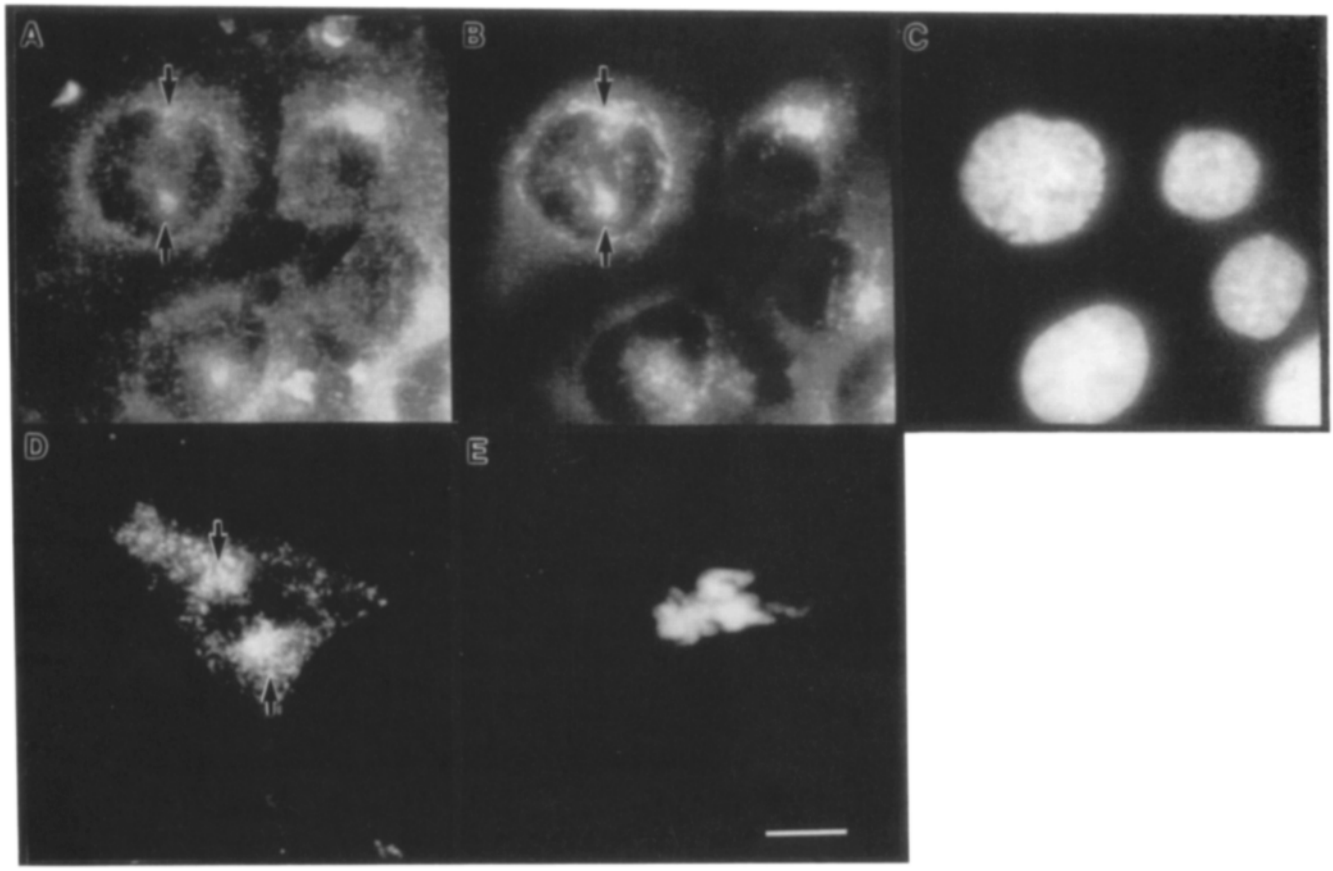

Figure 4. Co-staining of p60$^{c\text{-}src}$ and CI-MPR at the spindle poles of mitotic cells. *A–C* represent projections of the same RTCS fibroblast prophase cell stained with mAb 327 against p60$^{c\text{-}src}$ (*A*), anti-sera against CI-MPR (*B*) and Hoechst stain (*C*) to reveal the chromatin. Projections were obtained of Rat-1 fibroblasts stained with mAb 327 against p60$^{c\text{-}src}$ plus a sandwich antibody (see legend to Fig. 1; *D*) and with Hoechst stain to reveal the chromatin (*E*). Arrows indicate peri-centriolar staining in mitotic cells. Bar, 10 μm.

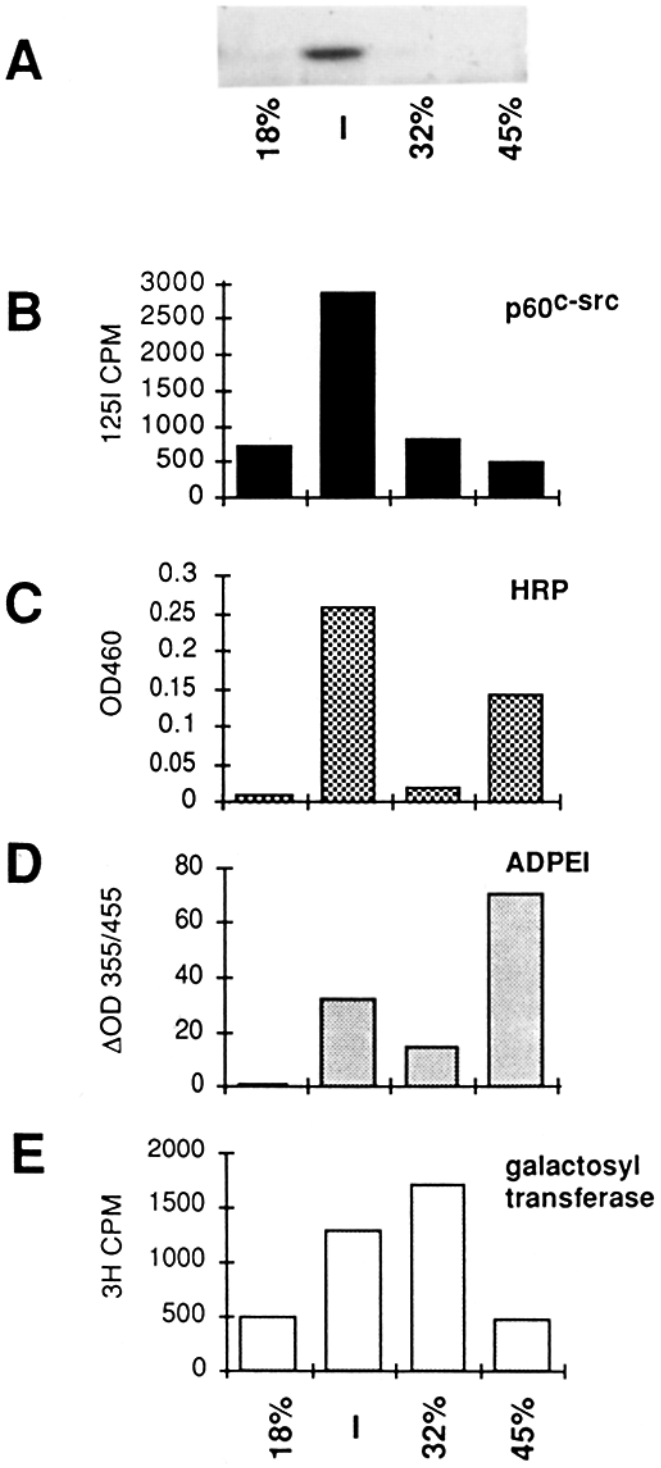

Figure 5. Enrichment of p60$^{c\text{-}src}$ and endosomal membranes on sucrose step gradients. RTCS fibroblasts were incubated with HRP for 30 min at 37°C and cell membranes were isolated and loaded on the bottom of a sucrose step gradient (see Materials and Methods). After centrifugation, fractions were analyzed by immunoblot with mAb 327 detected by ^{125}I labeled goat anti-mouse antibodies (*A*). Bands were cut from the blot and counted (*B*). Fractions were also analyzed for HRP activity (endosomal marker) (*C*), ADPE I activity (plasma membrane marker) (*D*), and galactosyl transferase activity (*cis/medial*-Golgi marker) (*E*).

tions remained in the supernatant and was therefore presumed to be soluble. In addition, treatment of cellular membranes with a water soluble, membrane impermeable cross-linking reagent (DTSSP) prevented the appearance of p60$^{c\text{-}src}$ in the 45 or 32% fractions, and resulted in a corresponding increase in the amount of p60$^{c\text{-}src}$ at the 18/32% interface. We therefore suspect that under normal homogenization conditions a minor fraction of p60$^{c\text{-}src}$ dissociates from cellular membranes and sediments near the bottom of the sucrose gradient.

We were particularly interested in separating plasma membranes and endosomal membranes because of the reported association of p60$^{c\text{-}src}$ with plasma membranes (Courtneidge et al., 1980). To further separate membranes, material from the 18/32% interface of the sucrose gradient was run on a percoll gradient and fractions were analyzed for the presence of p60$^{c\text{-}src}$. In multiple experiments, p60$^{c\text{-}src}$ migrated as a single peak in the low density fractions and paralleled the endocytic marker (HRP) profile (e.g., Fig. 6, *A* and *B*). In similar but separate experiments with total cellular membranes, p60$^{c\text{-}src}$ was also detected in low density fractions (data not shown) while Golgi markers, iodinated plasma membrane proteins (Fig. 6 *C*) and lysosomal markers (data not shown) were not enriched in p60$^{c\text{-}src}$-containing fractions. To rule out the possibility that soluble p60$^{c\text{-}src}$ present in cell homogenates was simply associating with endosomal membranes during cell lysis, we mixed p60$^{c\text{-}src}$ found in S100 fractions with membranes from cells not expressing p60$^{c\text{-}src}$ (due to a homozygous mutation at the src gene). P60$^{c\text{-}src}$ did not associate with endosomal membranes under these conditions, indicating that soluble p60$^{c\text{-}src}$ does not preferentially associate with endosomal membranes after cell lysis (data not shown).

Shift in Density of Endocytic Membranes Alters Membrane-Bound p60$^{c\text{-}src}$ Density

To determine if p60$^{c\text{-}src}$ is directly associated with endocytic vesicles inside the cell we specifically altered the density of endocytic membranes as described previously (Courtoy et al., 1984; Stoorvogel et al., 1991). Cells were allowed to internalize HRP to saturate the endocytic compartment (see Materials and Methods). Cellular membranes were isolated and sedimented on a sucrose step gradient as above. The 18/32% interface was isolated and split equally. Half of the interface membranes were treated with DAB and hydrogen peroxide (H_2O_2), a substrate and catalyst for HRP. The modification of DAB by HRP in endocytic vesicles results in an increase in vesicle density. Each set of membranes was analyzed on separate sucrose step gradients for the presence of p60$^{c\text{-}src}$ and HRP activity. As expected, DAB and H_2O_2 treatment resulted in a shift of the endocytic marker HRP to the 45% fraction (Fig. 7 *B*). Treatment of membranes with DAB and H_2O_2 also resulted in a shift of membranes containing p60$^{c\text{-}src}$ (Fig. 7 *A*) and CI-MPR (data not shown) to the 45% fraction. Other membrane markers present in the 18/32% interface did not undergo a shift in density to the 45% fraction after treatment with DAB (Fig. 7, *C* and *D*). The variation in the distribution of the Golgi marker galactosyl transferase (Fig. 7 *D*) was found to be dependent on homogenization conditions rather than DAB treatment, suggesting that the DAB-induced density shift was specific for

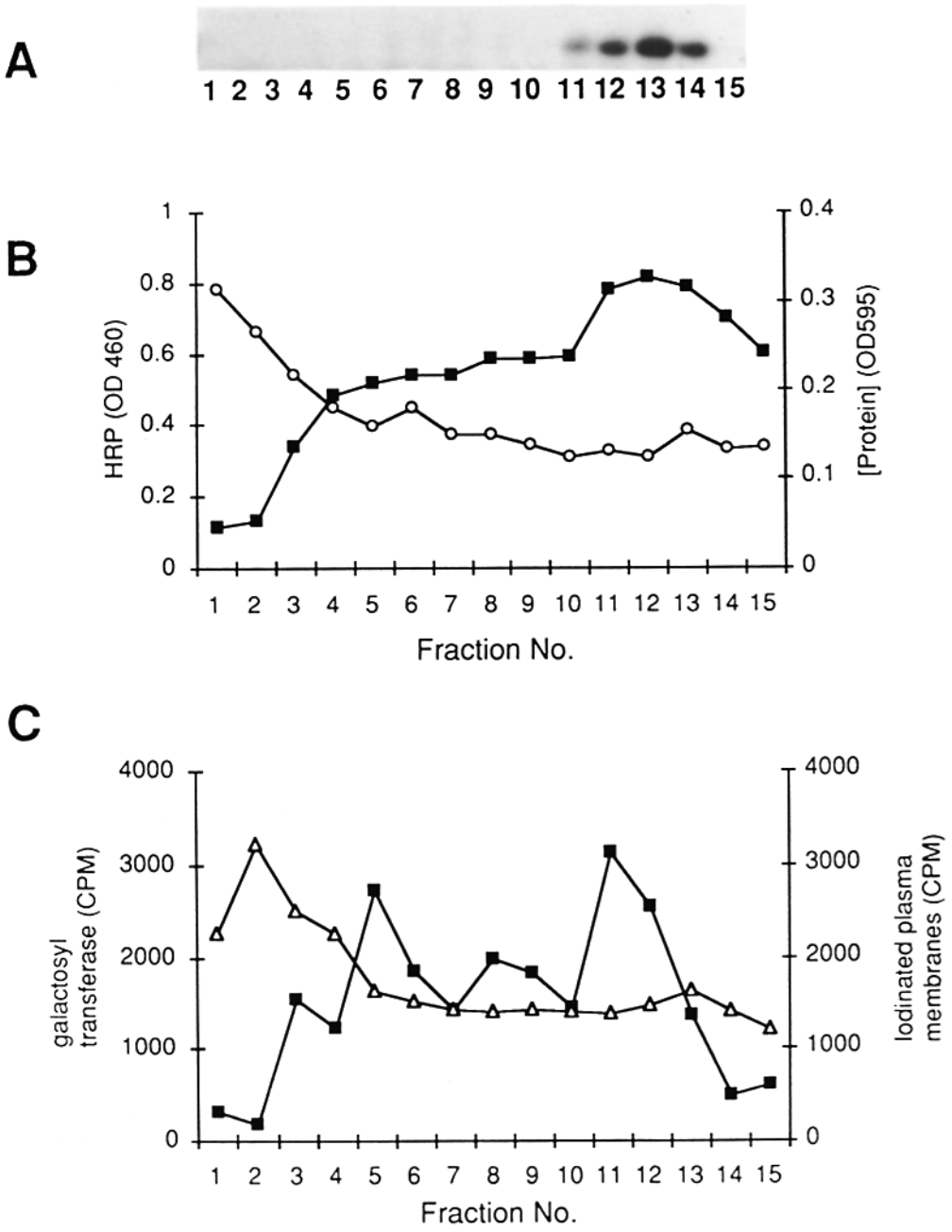

Figure 6. Separation of p60$^{c\text{-}src}$ from plasma membranes on percoll gradients. RTCS fibroblasts were incubated with HRP and cell membranes from the 18/32% interface of a sucrose step gradient were isolated and loaded on a percoll gradient (in the absence of $CaCl_2$; see Materials and Methods). Fractions were collected from the bottom of the gradient (1 = highest density and 15 = lowest density) and analyzed by immunoblot with mAb 327 against p60$^{c\text{-}src}$ (*A*), for protein concentration (*B*, ○) and HRP activity (*B*, ■). Whole cellular membranes from a p100 fraction were isolated in homogenization buffer (+2 mM $CaCl_2$; see Materials and Methods), run on parallel percoll gradients, analyzed for the Golgi marker galactosyl transferase (*C*, ■), and a gamma counter was used to detect the presence of iodinated plasma membrane proteins (*C*, △). The addition of $CaCl_2$ to the homogenization buffer in this experiment (see Materials and Methods; Fig. 6 *C*) further separated iodinated plasma membrane proteins from endosomal membranes by altering the apparent density of plasma membranes on the percoll gradient (Stoorvogel et al., 1989).

endosomal membranes. To demonstrate dependence of the density shift on the HRP reaction, samples treated only with DAB (or only with H_2O_2, data not shown) exhibited no shift in the apparent density of p60$^{c\text{-}src}$-associated membranes (Fig. 7 *A*, *left*).

Association of the Majority of p60$^{c\text{-}src}$ with Endosomal Membranes

All of the p60$^{c\text{-}src}$ isolated from the 18/32% fraction shifted density in these experiments, suggesting that all of the p60$^{c\text{-}src}$ in this fraction is associated with membranes accessible to the endocytic marker HRP. To determine the amount of p60$^{c\text{-}src}$ in the entire cell that is associated with endosomal membranes, we performed density shift experiments on the entire population of cellular membranes isolated from a 100,000 *g* pellet. The proportion of p60$^{c\text{-}src}$ in this pellet that undergoes a density shift should represent the proportion of membrane-bound p60$^{c\text{-}src}$ associated with endocytic membranes. After treatment with DAB and H_2O_2, total cellular membranes were separated on a percoll gradient and fractions were analyzed to identify p60$^{c\text{-}src}$ and relevant membrane markers. P60$^{c\text{-}src}$ from untreated membranes paralleled the peak of endosomal membranes (HRP) in low density fractions (Fig. 8 *A*). Treatment of membranes with DAB and H_2O_2 shifted the density of all detectable p60$^{c\text{-}src}$ and the endocytic marker HRP to higher density fractions (Fig. 8, *B* and *C*).

The shift in density of all detectable p60$^{c\text{-}src}$ suggested that the majority of p60$^{c\text{-}src}$ is associated with endosomal membranes and little or no p60$^{c\text{-}src}$ is associated with

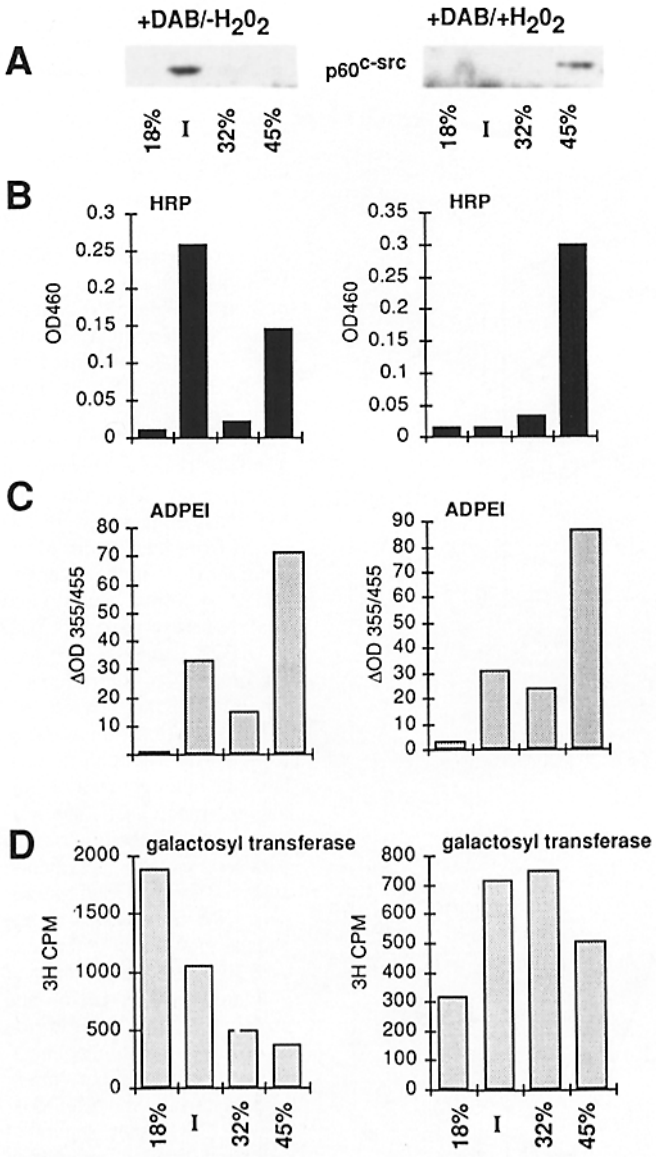

Figure 7. DAB-induced density shift of p60$^{c\text{-}src}$ in HRP-containing endosomes. Material from the 18/32% interface of a sucrose step gradient was treated with DAB in the presence (*right*) or absence (*left*) of H_2O_2. P60$^{c\text{-}src}$ was detected by immunoprecipitation and immunoblotting with mAb 327 (*A*). Fractions were also analyzed for HRP activity (*B*), ADPE I activity (plasma membrane marker) (*C*), and galactosyl transferase activity (*cis/medial*-Golgi marker) (*D*).

plasma membranes. However, it was possible that HRP bound to the plasma membrane was incorporated into vesicles, resulting in a shift in density of plasma membranes after DAB/H_2O_2 treatment. To address this possibility, attempts were made to determine the fate of plasma membranes after DAB/H_2O_2 treatment. Identification of plasma membranes by the measurement of enzymatic markers was impeded by low enzymatic activities in percoll. Instead, HRP-containing cells were surface iodinated at 0°C to identify plasma membranes. Measurement of ^{125}I after density shift revealed that there was no detectable shift in labeled plasma membrane proteins, while the p60$^{c\text{-}src}$-associated membranes underwent a shift in density as expected (Fig. 8). To further address the specificity of the density shift, HRP was bound to the surface of cells at 0°C to prevent endocytosis and cell membranes were harvested and treated with DAB and H_2O_2. No detectable density shift of p60$^{c\text{-}src}$ was observed (data not shown) despite high levels of HRP activity in the membrane pellet. Thus, only HRP internalized into the endocytic pathway is able to shift the density of p60$^{c\text{-}src}$-containing membranes.

It was also possible that there was a preferential solubilization of plasma membrane-associated p60$^{c\text{-}src}$ during preparation of cellular membranes. The ~10–20% of total p60$^{c\text{-}src}$ that we detected in the soluble S100 fraction may therefore represent a plasma membrane-associated fraction of p60$^{c\text{-}src}$. To address this possibility, cell extracts were treated with DTSSP (as described above) to reduce the amount of p60$^{c\text{-}src}$ in the S100 fraction. P60$^{c\text{-}src}$ was fractionated on percoll gradients and did not cosediment with plasma membranes (data not shown). It is therefore unlikely that the population of soluble p60$^{c\text{-}src}$ came from the plasma membrane.

Discussion

We have found that the majority of membrane-associated p60$^{c\text{-}src}$ in mammalian fibroblasts is localized to a compartment that probably represents a population of endosomes. Our immunofluorescence experiments demonstrate that a significant proportion of p60$^{c\text{-}src}$ is found at the MTOC and co-localizes with CI-MPR, a marker of late endosomes. Biochemical fractionation and density shift experiments indicate that the majority of p60$^{c\text{-}src}$ in the cell associates with endosomal membranes accessible to the endocytic marker HRP. These results raise the possibility that p60$^{c\text{-}src}$ plays a role in endosomal function.

Previous immunofluorescence and electron microscopic studies of p60$^{v\text{-}src}$ tend to support localization of the viral src protein at the plasma membrane (Rohrschneider, 1979; Willingham et al., 1979). Some src family members are thought to interact with cell surface proteins, and a putative plasma membrane receptor for p60$^{v\text{-}src}$ has been identified in cross-linking experiments (Resh and Ling, 1990). In contrast, our results suggest that very little p60$^{c\text{-}src}$ is associated with plasma membranes. Although we sometimes observed p60$^{c\text{-}src}$ staining at cell–cell contacts, we suspect that this does not represent plasma membrane association but rather is because of enrichment of membranes at bundles of microtubules (Fig. 1). Dependence on intact microtubules for this localization further supports the notion that p60$^{c\text{-}src}$ is microtubule-associated at cell–cell contacts. The discrepancy between previous localization studies and our results may arise in part from differences between the transforming protein p60$^{v\text{-}src}$ and the nontransforming protein p60$^{c\text{-}src}$.

Our results also differ from previous studies that have used biochemical fractionation to localize src proteins. These studies demonstrate an enrichment of both p60$^{v\text{-}src}$ and p60$^{c\text{-}src}$ in plasma membranes (Courtneidge et al., 1980; Resh and Erikson, 1985). Fractionation techniques used in these studies did not differentiate between plasma membranes and endosomal membranes, which have similar densities and are likely to cosediment. We have used variable conditions during homogenization to alter the sedimentation of plasma membranes, allowing them to be separated from endosomes

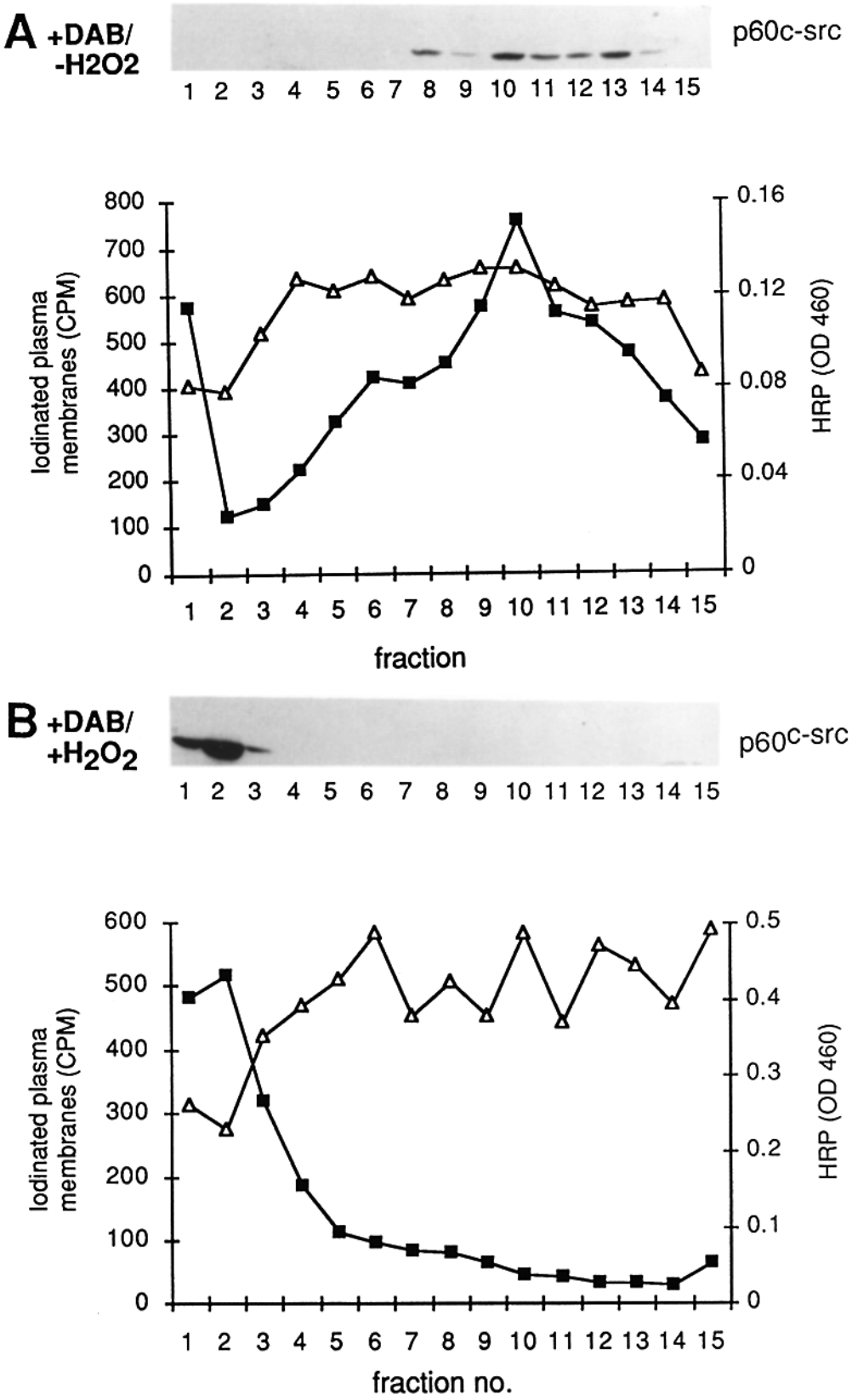

Figure 8. DAB-induced density shift of $p60^{c\text{-}src}$ from total cellular membranes. RTCS fibroblasts were incubated with HRP and total cellular membranes were isolated. Membranes were treated with DAB alone (*A*), or DAB/H_2O_2 (*B*) and then run on percoll gradients. Fractions were collected as in Fig. 6. $P60^{c\text{-}src}$ was detected by immunoprecipitation and immunoblotting with mAb 327. Fractions were also analyzed for HRP activity to detect endosomal membranes (■) and a gamma counter was used to detect the presence of iodinated plasma membrane proteins (△). Note that plasma membranes do not behave as in Fig. 6 due to the absence of $CaCl_2$ (see legend to Fig. 6).

(see Materials and Methods). In addition, the specific shift in density of HRP-containing membranes convincingly separated endosomes from plasma membranes. Based on results from these fractionation experiments we have concluded that no detectable $p60^{c\text{-}src}$ is associated with plasma membranes. It remains possible that a very small proportion of $p60^{c\text{-}src}$ is associated with plasma membranes but is undetectable under our conditions.

Our results suggest that p60$^{c\text{-}src}$ is associated with the microtubule cytoskeleton via endocytic vesicles, in contrast to previous localization and biochemical studies suggesting an association of p60$^{v\text{-}src}$ with the actin cytoskeleton (Hamaguchi and Hanafusa, 1987; Henderson and Rohrschneider, 1987; Resh and Erickson, 1985; Rohrschneider, 1979, 1980). Analysis of optical sections near the bottom of cells over-expressing chicken p60$^{c\text{-}src}$ showed only punctate, microtubule-associated staining and no localization to adhesion plaques. We found that p60$^{c\text{-}src}$ co-localizes with a number of microtubule-related structures, including microtubule bundles at points of cell–cell contact, the microtubule organizing center, and a region associated with the spindle pole during mitosis (Figs. 1 and 4). In all cases this staining is dependent on intact microtubules. Ample evidence has demonstrated that endocytic membranes can be transported along microtubules (DeBrabander et al., 1988; Goergi et al., 1990; Matteoni and Kreis, 1987). It is therefore likely that co-localization of p60$^{c\text{-}src}$ with various microtubule structures reflects the transport of endosomal membranes along cellular microtubules. It is even conceivable that p60$^{c\text{-}src}$ may regulate microtubules or microtubule-associated motors involved in endosomal membrane transport.

The microtubule-dependent alteration of p60$^{c\text{-}src}$ staining induced by BFA treatment provides additional evidence for p60$^{c\text{-}src}$ transport along microtubules. BFA is known to cause microtubule-dependent retrograde transport of Golgi elements into the ER (Lippincott-Schwartz et al., 1989, 1990). We have shown that treatment of cells with BFA also affects the transport of endosomal membranes containing p60$^{c\text{-}src}$. BFA treatment results in the clustering of p60$^{c\text{-}src}$-containing membranes at the centrosome, which is distinct from the normally diffuse staining of p60$^{c\text{-}src}$ at the MTOC (Fig. 3). Similar findings have been reported for the effect of BFA on a wide range of endocytic membranes in both rat and canine cells (Lippincott-Schwartz et al., 1991; Wood et al., 1991). While the mechanism of action of BFA remains unclear, the behavior of p60$^{c\text{-}src}$ and CI-MPR after BFA treatment emphasizes the similar nature of the membrane compartment occupied by these proteins.

Studies of cells in early stages of mitosis show that p60$^{c\text{-}src}$ and CI-MPR are found at the dividing centrosomes (Fig. 4). The presence of both CI-MPR and p60$^{c\text{-}src}$ at the spindle poles during mitosis further suggests that both of these proteins reside in a similar membrane compartment that is distinct from *cis/medial*-Golgi membranes, which are scattered throughout the cell during mitosis (K. Kaplan, unpublished observations) (Lucocq and Warren, 1987; Moskalewski and Thyberg, 1990). Since p60$^{c\text{-}src}$ is known to be activated during mitosis and phosphorylated by p34^{cdc2} (Chackalaparampil and Shalloway, 1988; Morgan et al., 1989), it is possible that p60$^{c\text{-}src}$ is mediating mitotic effects of p34^{cdc2} at the pericentriolar region of the cell. Several processes associated with endosomal membranes are known to be regulated during mitosis. For example, it has been shown in vitro that early endosomal fusion events are inhibited by addition of active *Xenopus* p34^{cdc2} (Tuomikoski et al., 1989; Woodman et al., 1992).

Work with secretory cells suggests that p60$^{c\text{-}src}$ may be involved in regulating the function of specialized secretory vesicles. In addition to being enriched in secretory granules of chromaffin cells, p60$^{c\text{-}src}$ is associated with a 38-kD protein that may be important in the function of these secretory organelles (Grandori and Hanafusa, 1988). These compartments may be analogous to the endosomal compartment in fibroblasts. The association of p60$^{c\text{-}src}$ with endosomally derived synaptic vesicles in PC-12 cells is consistent with this proposal (Johnston et al., 1989; Linstedt et al., 1992).

Endosomal membranes are dynamic structures involved in the trafficking of proteins throughout the cell and are known to be regulated at the level of both transport and fusion. In this regard it may be relevant to consider the phenotype of mice that are genetically null for the c-src gene through homologous recombination (Soriano et al., 1991). The defect in bone modeling (osteopetrosis) exhibited by these mice arises ultimately from an inability to dissolve bone tissue during development. The osteoclasts responsible for dissolving bone tissue are known to be highly specialized secretory cells that secrete lysosomal enzymes. In the absence of p60$^{c\text{-}src}$ these cells may be defective in regulating the trafficking of lysosomal proteins.

We would like to thank David Agard and John Sedat for the use of their microscopy facilities, Peter Lobel and William Brown for antisera against the CI-MPR, Josh Kaplan for the RTCS cell line, and Phil Soriano for mouse embryo fibroblasts from transgenic mice. We are grateful to members of the Src group and Frances Brodsky for helpful discussions and to Inke Näthke and John Young for valuable comments on the manuscript.

This work was supported by grants to D. O. Morgan and H. E. Varmus from the National Institutes of Health, a Searle Scholars Award from the Chicago Community Trust (D. O. Morgan) and a Basil O'Connor Starter Scholar Award from the March of Dimes Birth Defects Foundation (D. O. Morgan). H. E. Varmus is an American Cancer Society Research Professor.

Received for publication 31 January 1992 and in revised form 4 April 1992.

References

Agard, D. A., P. Hiraoka, P. Shaw, and J. W. Sedat. 1989. Fluorescence microscopy in three dimensions. *Methods Cell Biol.* 30:353–377.

Aoki, D., H. E. Apperti, D. Johnson, S. S. Wong, and M. N. Fukada. 1990. Analysis of the substrate binding sites of human galactosyl transferase by protein engineering. *EMBO (Eur. Mol. Biol. Organ.) J.* 9:3171–3178.

Bole, D. G., L. M. Hendershot, and J. F. Kearney. 1989. Post-translational association of immunoglobulin heavy chain binding protein with nascent heavy chains in nonsecreting hybridomas. *J. Cell Biol.* 102:1558–1566.

Buss, J. E., and B. M. Sefton. 1985. Myristic acid, a rare fatty acid, is the lipid attached to the transforming protein of Rous sarcoma virus and its cellular homolog. *J. Virol.* 53:7–12.

Buss, J. E., M. P. Kamps, K. Gould, and B. M. Sefton. 1986. The absence of myristic acid decreases membrane binding of p60^{src} but does not affect tyrosine protein kinase activity. *J. Virol.* 58:468–474.

Chackalaparampil, I., and D. Shalloway. 1988. Altered phosphorylation and activation of pp60$^{c\text{-}src}$ during fibroblast mitosis. *Cell.* 52:801–810.

Chege, W. N., and S. R. Pfeffer. 1990. Compartmentation of the golgi complex: brefeldin-A distinguishes trans-golgi cisternae from the trans-golgi network. *J. Cell Biol.* 111:893–899.

Cooper, J. A. 1989. The src-family of protein-tryosine kinases. *In* Peptides and Protein Phosphorylation. B. Kemp and P. F. Alewood, editors. CRC Press, Boca Raton, FL. 85–113.

Cotton, P. C., and J. S. Brugge. 1983. Neural tissues express high levels of the cellular src gene product pp60$^{c\text{-}src}$. *Mol. Cell. Biol.* 3:1157–1162.

Courtneidge, S. A., A. D. Levinson, and J. M. Bishop. 1980. The protein encoded by the transforming gene of avian sarcoma virus (pp60^{src}) and a homologous protein in normal cells (pp60$^{proto\text{-}src}$) are associated with the plasma membrane. *Proc. Natl. Acad. Sci. USA.* 77:3783–3787.

Courtoy, P. J., J. Quintart, and P. Baudhuin. 1984. Shift of equilibrium density induced by 3,3'-diaminobenzidine cytochemistry: a new procedure for the analysis and purification of peroxidase-containing organelles. *J. Cell Biol.* 98:870–876.

David-Pfeuty, T., and Y. Nouvian-Dooghe. 1990. Immunolocalization of the cellular src protein in interphase and NIH c-src overexpressor cells. *J. Cell Biol.* 111:3097–3116.

DeBrabander, M., R. Nuydens, H. Geerts, and C. R. Hopkins. 1988. Dynamic behavior of the transferrin receptor followed in living epidermoid carcinoma

(A431) cells with nonovid microscopy. *Cell Motil. Cytoskeleton.* 9:30–47.
Goergi, A., C. Mottola-Harthshorn, A. Warner, B. Fields, and L. B. Chen. 1990. Detection of individual fluorescently labeled reovirions in living cells. *Proc. Natl. Acad. Sci. USA.* 87:6579–6583.
Golden, A., S. P. Nemeth, and J. S. Brugge. 1986. Blood platelets express high levels of pp60$^{c\text{-}src}$ specific tyrosine kinase activity. *Proc. Natl. Acad. Sci. USA.* 83:852–856.
Grandori, C., and H. Hanafusa. 1988. P60$^{c\text{-}src}$ is complexed with a cellular protein in subcellular compartments involved in exocytosis. *J. Cell Biol.* 107:2125–2135.
Hamaguchi, M., and H. Hanafusa. 1987. Association of p60^{src} with Triton X-100-resistant cellular structure correlates with morphological transformation. *Proc. Natl. Acad. Sci. USA.* 84:2312–2316.
Harlow, E., and D. Lane. 1988. Antibodies: A Laboratory Manual. Cold Spring Harbor Laboratory, Cold Spring Harbor, NY. 726 pp.
Henderson, D., and L. Rohrschneider. 1987. Cytoskeletal association of pp60^{src}, the transforming protein of the Rous sarcoma virus. *Exp. Cell Res.* 168:411–421.
Hiraoka, Y., D. A. Agard, and J. W. Sedat. 1990. Temporal and spatial coordination of chromosome movement, spindle formation, and nuclear envelope breakdown during prometaphase in *Drosophila melanogaster* embryos. *J. Cell Biol.* 111:2815–2828.
Hiraoka, Y., J. R. Swedlow, M. R. Paddy, D. A. Agard, and J. W. Sedat. 1991. Three-dimensional multiple wavelength microscopy for the structural analysis of biological phenomena. *Sem. Cell Biol.* 2:153–165.
Johnston, P. A., P. L. Cameron, H. Stukenbrok, R. Jahn, P. De Camilli, and T. C. Sudhof. 1989. Synaptophysin is targeted to similar microvesicles in CHO and PC12 cells. *EMBO (Eur. Mol. Biol. Organ.) J.* 8:2863–2872.
Kamps, M. P., J. E. Buss, and B. M. Sefton. 1986. Rous sarcoma virus transforming protein lacking myristic acid phosphorylates known polypeptide substrates without inducing transformation. *Cell.* 45:105–112.
Kaplan, J. M., H. E. Varmus, and J. M. Bishop. 1990. The src protein contains multiple domains for specific attachment to membranes. *Mol. Cell Biol.* 10:1000–1009.
Lewis, V., S. A. Green, M. Marsh, P. Vihko, A. Helenius, and I. Mellman. 1985. Glycoproteins of the lysosomal membrane. *J. Cell Biol.* 100:1839–1847.
Linstedt, L. D., M. L. Vetter, J. M. Bishop, and R. B. Kelly. 1992. Specific association of the proto-oncogene product pp60$^{c\text{-}src}$ with intracellular organelle, the PC12 synaptic vesicle. *J. Cell Biol.* 117:1077–1084.
Lippincott-Schwartz, J., L. C. Yuan, J. S. Bonifacino, and R. D. Klausner. 1989. Rapid redistribution of golgi proteins into the ER in cells treated with Brefeldin A: evidence for membrane cycling from golgi to ER. *Cell.* 56: 801–813.
Lippincott-Schwartz, J., J. G. Donaldson, A. Schweizer, E. G. Berger, H.-P. Hauri, L. C. Yuan, and R. D. Klausner. 1990. Microtubule-dependent retrograde transport of proteins into the ER in the presence of Brefeldin A suggests an ER recycling pathway. *Cell.* 60:821–836.
Lippincott-Schwartz, J., L. Yuan, C. Tipper, M. Amherdt, L. Orci, and R. D. Klausner. 1991. Brefeldin A's effect on endosomes, lysosomes and the TGN: a general mechanism for regulating organelle structure and membrane traffic. *Cell.* 67:601–616.
Lipsich, L. A., A. J. Lewis, and J. S. Brugge. 1983. Isolation of monoclonal antibodies that recognize the transforming proteins of avian sarcoma virus. *J. Virol.* 48:352–360.
Lucocq, J. M., and G. Warren. 1987. Fragmentation and partitioning of the Golgi apparatus during mitosis in Hela cells. *EMBO (Eur. Mol. Biol. Organ.) J.* 6:3239–3246.
Matteoni, R., and T. E. Kreis. 1987. Translocation and clustering of endosomes and lysosomes depends on microtubules. *J. Cell Biol.* 105:1253–1265.
Messner, D. J., G. Griffiths, and S. Kornfeld. 1989. Isolation and characterization of membranes from bovine liver which are highly enriched in mannose 6-phosphate receptors. *J. Cell Biol.* 108:2149–2162.
Morgan, D. O., J. M. Kaplan, J. M. Bishop, and H. E. Varmus. 1989. Mitosis-specific phosphorylation of p60$^{c\text{-}src}$ by p34^{cdc2}-associated protein kinase. *Cell.* 57:775–786.
Morgan, D. O., J. M. Kaplan, J. M. Bishop, and H. E. Varmus. 1991. Production of p60$^{c\text{-}src}$ by baculovirus expression and immuno-affinity purification. *Methods Enzymol.* 200:645–660.
Moskalewski, S., and J. Thyberg. 1990. Disorganization and reorganization of the golgi complex and the lysosomal system in association with mitosis. *J. Submicrosc. Cytol. Pathol.* 22:159–171.
Paddy, M. R., A. S. Belmont, H. Saumweber, D. A. Agard, and J. W. Sedat. 1990. Interphase nuclear envelope lamins form a discontinuous network that interacts with only a fraction of the chromatin in the nuclear periphery. *Cell.* 62:89–106.
Poole, R. R. J., K. M. Maurey, and B. Storrie. 1983. Characterization of pinocytic vesicles from CHO cells: resolution of pinosomes from lysosomes by analytical centrifugation. *Cell Biol. Int. Rep.* 7:361–367.
Resh, M. D., and R. L. Erikson. 1985. Highly specific antibody to Rous sarcoma virus src gene product recognizes a novel population of pp60$^{v\text{-}src}$ and pp60$^{c\text{-}src}$ molecules. *J. Cell Biol.* 100:409–417.
Resh, M. D., and H. Ling. 1990. Identification of a 32K plasma membrane protein that binds to the myristylated amino-terminal sequence of p60$^{v\text{-}src}$. *Nature (Lond.).* 346:84–86.
Rohrschneider, L. R. 1979. Immunofluorescence on avian sarcoma virus-transformed cells: localization of the src gene product. *Cell.* 16:11–24.
Rohrschneider, L. R. 1980. Adhesion plaques of Rous sarcoma virus-transformed cells contain the src gene product. *Proc. Natl. Acad. Sci. USA.* 77: 3514–3518.
Shenoy, S., J. K. Choi, S. Bagrodia, T. D. Copeland, J. L. Maller, and D. Shalloway. 1989. Purified maturation promoting factor phosphorylates pp60$^{c\text{-}src}$ at the sites phosphorylated during fibroblast mitosis. *Cell.* 57: 761–772.
Soriano, P., C. Montgomery, R. Geske, and A. Bradley. 1991. Targeted disruption of the c-src proto-oncogene leads to osteopetrosis in mice. *Cell.* 64: 693–702.
Stoorvogel, W., H. J. Geuze, J. M. Griffith, A. L. Schwartz, and G. J. Strous. 1989. Relations between the intracellular pathways of the receptors for transferrin, asialoglycoprotein, and mannose 6-phosphate in human hepatoma cells. *J. Cell Biol.* 108:2137–2148.
Stoorvogel, W., G. J. Strous, H. J. Geuze, V. Oorschot, and A. L. Schwartz. 1991. Late endosomes derive from early endosomes by maturation. *Cell.*65: 417–427.
Thompson, J. A., A. L. Lau, and D. D. Cunningham. 1987. Selective radiolabeling of cell surface proteins to a high specific activity. *Biochemistry.* 26: 743–750.
Tuomikoski, T., M.-A. Felix, M. Doree, and J. Gruenberg. 1989. Inhibition of endocytic vesicle fusion *in vitro* by the cell cycle control protein kinase cdc2. *Nature (Lond.).* 342:942–945.
Willingham, M. C., G. Jay, and I. Pastan. 1979. Localization of the ASV src gene product to the plasma membrane of transformed cells by electron microscopic immunocytochemistry. *Cell.* 18:125–134.
Wood, S. A., J. E. Park, and W. J. Brown. 1991. Brefeldin A causes a microtubule-mediated fusion of the trans-golgi network and early endosomes. *Cell.* 67:591–600.
Woodman, P. G., D. I. Mundy, P. Cohen, and G. Warren. 1992. Cell-free fusion of endocytic vesicles is regulated by phosphorylation. *J. Cell Biol.* 116: 331–338.